ACS APPLIED ENERGY MATERIALS

Universitat d'Alacant
Universidad de Alicante

Subscriber access provided by Universidad de Alicante

Article

The Use of CO as Cleaning Tool of Highly Active Surfaces in Contact with Ionic Liquids. Ni Deposition on Pt(111) Surfaces in IL

PAULA SEBASTIAN, Michal Tulodziecki, María del Pilar Bernicola, Victor Climent, Elvira Gómez, Yang Shao-Horn, and Juan M. Feliu

ACS Appl. Energy Mater., **Just Accepted Manuscript** • DOI: 10.1021/acsaem.8b00776 • Publication Date (Web): 20 Aug 2018

Just Accepted

ACS Publications

is published by the American Chemical Society. 1155 Sixteenth Street N.W., Washington, DC 20036

The Use of CO as Cleaning Tool of Highly Active Surfaces in Contact with Ionic Liquids. Ni Deposition on Pt(111) Surfaces in IL

P. Sebastian[†], M. Tułodziecki[‡], M.P. Bernicola[†], V. Climent[†], E. Gómez[§], Y. Shao-Horn[‡,∥,⊥], J.M. Feliu[†]**

† Instituto de Electroquímica, Universidad de Alicante, Apartado 99, E-03080, Alicante, Spain.

‡ Research Laboratory of Electronics, Massachusetts Institute of Technology, 77 Massachusetts Ave., Cambridge, MA, 02139 USA

§ Departament Ciència de Materials i Química Física and Institut de Nanociència i Nanotecnologia (IN2UB), Universitat de Barcelona, 08028 Barcelona, Spain

∥ Department of Mechanical Engineering, Massachusetts Institute of Technology, 77 Massachusetts Ave., Cambridge, MA, 02139 USA

⊥ Department of Materials Science and Engineering, Massachusetts Institute of Technology, 77 Massachusetts Ave., Cambridge, MA, 02139 USA

Corresponding Author

*E-mail: paula.sebastian@ua.es

*E-mail: juan.feliu@ua.es

KEYWORDS

Room Temperature Ionic Liquid, Deep Eutectic Solvent, Carbon monoxide oxidation, Interfacial water, Phase transition, Nickel electrodeposition.

ABSTRACT

This work proposes a pretreatment strategy of a flame-annealed Pt(111) single crystal ensuring surface ordering and avoiding water surface contamination for experiments in ionic liquid (IL) media. A room temperature ionic liquid (RTIL) and a Deep Eutectic Solvent (DES) representative of two families of ionic liquids were selected as test electrolytes: The RTIL used was the 1-ethyl-2,3-dimethylimidazolium bis(trifluoromethyl)sulfonylimide ([Emmim][Tf_2N]) and the DES was based on the eutectic mixture of choline chloride (ChCl) and urea (1ChCl:2urea molar ratio). The electrode was flame-annealed and, instead of the water quenching step, it was cooled down in CO atmosphere until the surface was fully covered by a protective carbon monoxide (CO) layer. Prior to experiments, the removal of CO from the surface was performed by electrochemical oxidation. The CO reactivity on Pt(111) was different depending on the IL nature. While CO is easily oxidised to CO_2 in [Emmim][Tf_2N], in DES CO remains adsorbed on the substrate and restructures undergoing an order-disorder transition. For both liquids, the proposed method allows obtaining neat blank cyclic voltammograms, demonstrating that the adsorption of CO is a useful tool to protect the high catalytic surfaces such as Pt in contact with ILs.

To illustrate the feasibility of the CO treatment in electrochemical work with ILs, the general trends for the modification of Pt(111) single crystal surface with metallic nickel nanostructures on both types of IL was investigated. Nickel electrodeposition on the Pt(111) substrate was explored in both [Emmim][Tf_2N] and

DES by using classical electrochemical techniques such as cyclic voltammetry and chronoamperometry, while the deposits were characterized by FE-SEM, EDS and XPS.

INTRODUCTION

The incorporation of Ionic Liquids (ILs) as novel electrolytes for many reactions of interest in electrochemistry has motivated the study of their interactions with highly active materials such as Pt, Ir or their alloys. These metals show different activity depending on their crystallographic orientation[1-3]. For this reason, a deeper understanding of the properties of well-defined Pt(hkl)|IL interfaces is demanded. However, there are a few publications devoted on investigating the Pt(hkl)|IL interfaces paying attention to the influence of the liquid structure[1-6]. Hence, strategies are needed to keep clean and ordered the Pt(hkl) surfaces in contact with the ILs. Platinum surfaces are highly reactive and contaminate easily (i.e., surface blockage), hindering the achieving of reproducible results, fact that could explain the lack of information related with platinum electrochemistry in IL media. Traditionally, the best methodology employed to pretreat a Pt single crystal electrode was the so-called flame annealing treatment introduced in 1980 by J. Clavilier, method that requires the quenching in water as the final step of the treatment[7]. This procedure is not convenient using an IL as a solvent because it would involve the attachment of water to the surface perturbing the electrochemical results. In the search of alternative methods, we have explored the use of carbon monoxide (CO) to protect the Pt(hkl) electrodes. CO is a neutral probe that adsorbs strongly on Pt and protects the surface from the surrounding atmosphere[8]. In aqueous electrolytes, CO can be easily removed from the surface by its electrochemical oxidation to CO_2 [8-12]. In the few reports devoted to the study of CO oxidation on Pt surfaces in contact with RTILs, authors have found that this reaction is dependent on two factors: the amount of water content in the RTIL and, particularly, the specific nature of the anion in the RTIL [6, 13]. These factors also determine the electrochemical stability of the RTIL (i.e the electrochemical window) and their availability to oxidize

CO with or without overlapping with solvent oxidation. In the present work, keeping in mind previous results obtained in ILs and aqueous media, CO blockage and oxidation was investigated and evaluated as a tool to maintain the cleanliness and to protect the Pt surfaces after the flame annealing and during the transfer to either [Emmim][Tf_2N] or DES solvents. A Pt(111) single crystal was employed as substrate.

As an evaluation of the feasibility of CO treatment in ILs, we have checked the Ni electrodeposition on Pt(111) surfaces pretreated with CO. Nickel electrodeposition on Pt(111) surfaces was explored as an example of a route to modify a high catalytic and well-ordered surface such as Pt(111) with foreign metal structures .Nickel is hardly deposited in aqueous electrolytes[14, 15]. The motivation to select the Ni among other metals to modify Pt substrates is the fact that Ni is a cheap and abundant metal which combination with Pt enhances the catalytic properties of the system for several reactions of interest[16-18].

EXPERIMENTAL SECTION

The RTIL [Emmim][Tf_2N] was purchased from Iolitec in the highest available quality (99% < 60ppm halides, < 60ppm water). The RTIL was then transferred to an argon glove box (Mbraun, USA, H_2O <1 ppm, O_2 <1%). Before carrying the experiments, around 1-2 mL of [Emmim][Tf_2N] were dried under vacuum (P<0.0025mPas), while heating (80ºC) and stirring conditions. Then, the stirring was stopped and activated molecular sieves (3Å) were added in order to remove residual water and impurities, according to the Kolb's procedure[19]. Afterwards, the water content in the RTIL was measured by Karl Fisher Tritation, measuring a value lesser than 10 ppm. The Ni[Tf_2N]$_2$ salt was purchased from Alfa Aesar in the highest quality available (98%). This salt was dried overnight under vacuum and high temperature conditions

(150ºC) before adding to the RTIL. The hydrated salt was initially blue and changed to yellow evidencing the loss of water. The prepared nickel concentration in the [Emmim][Tf_2N] was 0.05M.

Both the choline chloride (ChCl) and the urea were purchased in high purity quality (99%) from Merck. The DES corresponds to the eutectic mixture (1ChCl: 2urea) molar ration[20] and was prepared by mixing both components under a temperature not higher than 50ºC, until a liquid was obtained stable at room temperature. Then the liquid was transferred to a glass recipient connected to a vacuum pump and dried under vacuum (P<0.002mbar), stirring and heating conditions (T<50ºC) overnight. The water content, measured electrochemically, was around 1%. Ni(II) solution was prepared, from $NiCl_2{*}6H_2O$ salt of 99% purity grade from Merck. This salt was dried at 100ºC overnight. After that, a 0.1M Ni(II) solution in DES was prepared. In order to dissolve the nickel salt in the DES, the mixture was stirred during 24 h under vacuum and heating conditions (T<50ºC).

Suprapure $HClO_4$ from Merck was used for the CO oxidation tests in ultra-pure water aqueous solution.

The working electrode was a bead type Pt(111) pretreated by flame-annealing and cooled down under the presence of CO, until the surface was completely blocked by the CO[21].

A three-electrode cell was employed to carry out the experiments. As a reference electrode, a quasi-reference silver wire was used for the experiments carried in [Emmim][Tf_2N] being the potential referred to the Fc^+/Fc redox pair. In the DES, Ag|AgCl|DES reference electrode was used. In aqueous solutions, a reversible hydrogen electrode (RHE) was employed. As a counter electrode, a platinum wire spiral was employed in all cases. Experiments with [Emmim][Tf_2N] were carried at 25ºC inside a

glove box, while for the DES a thermostatized cell was employed, keeping the temperature at 70ºC. In addition, the electrochemical cell was always maintained under Ar atmosphere to minimize further hydration or organic contamination from the environment.

Either a Biologic potentiostat BP300 or a μ-Autolab GPES potentiostat were used to carry both cyclic voltammetric and chronoamperometric measurements. A JEOL JSM-7100F Analytical Microscopy Field Emission scanning electron microscope FE-SEM coupled with EDS spectroscopy was used to characterize the deposits. X-ray photoelectron spectroscopy (XPS) measurements were carried out with an K-ALPHA, Thermo Scientific. All spectra were collected using Al-K radiation (1486.6 eV).

RESULTS

CO reaction on Pt(111)|0.1M $HClO_4$ aqueous blank solution

Prior to investigating the Pt(111)|IL interface, the CO pretreatment was evaluated in a solution containing 0.1 M $HClO_4$. The electrode was flame-annealed and cooled down in CO atmosphere for enough time to ensure complete surface blockage, but no electrode quenching in water was carried out after the cooling down step. Figure 1A shows the cyclic voltammetry of the CO stripping on Pt(111)|0.1M $HClO_4$ interface after performing the pretreatment. At low potentials the absence of current evidences the full interface blockage. The main CO oxidation peak appears centred at 0.75 V vs RHE. Interestingly, the main peak is preceded by a small peak located at 0.64 V vs RHE, which origin could be related with the cooling treatment. Once the CO was oxidized, the Pt(111) displays the common blank cyclic voltammogram reported in 0.1M $HClO_4$. Figure 1B shows the CO stripping on Pt(111) after holding the covered

Pt(111) electrode in air, during 10 and 60 minutes respectively, overlapped with the CO stripping voltammetry from Figure 1A (in which the electrode was immediately introduced in the cell after the thermic treatment). The goal of these experiments is evaluating the efficiency of CO to keep the Pt(111) surface protected during long periods of time. After holding the electrode for 10 and 60 minutes the Pt(111) is still fully covered by CO, and the overall charge involved in the main CO oxidation peak hardly changes (about 360 μC cm^{-2} in all cases). The most interesting fact is that the small peak at 0.64 V recorded in Figure 1A, which involves a charge value of around 22 μC cm^{-2}, has disappeared from the voltammograms in which the covered Pt(111) electrode was held some time in air. This result suggests that the identity of the small peak would be related with weakly adsorbed CO on the surface[22, 23]. It is remarkable that, in the absence of electrolyte, the atmospheric oxygen is not able to oxidise the CO on the surface, even after such a long time. Figure 1C compares the blank cyclic voltammograms recorded after CO oxidation for the three previously described exposition times to the atmosphere after the CO pretreatment. Voltammograms are practically identical, except for a very small decrease in charge observed in the anion adsorption region (feature at 0.85 V). The loss in the recorded charge is nearly negligible, and therefore, the CO pretreatment is validated as a tool to keep the Pt(111) surface clean and ordered without using water quenching, especially taking into account that the transfer to the cell is lower than 5 minutes.

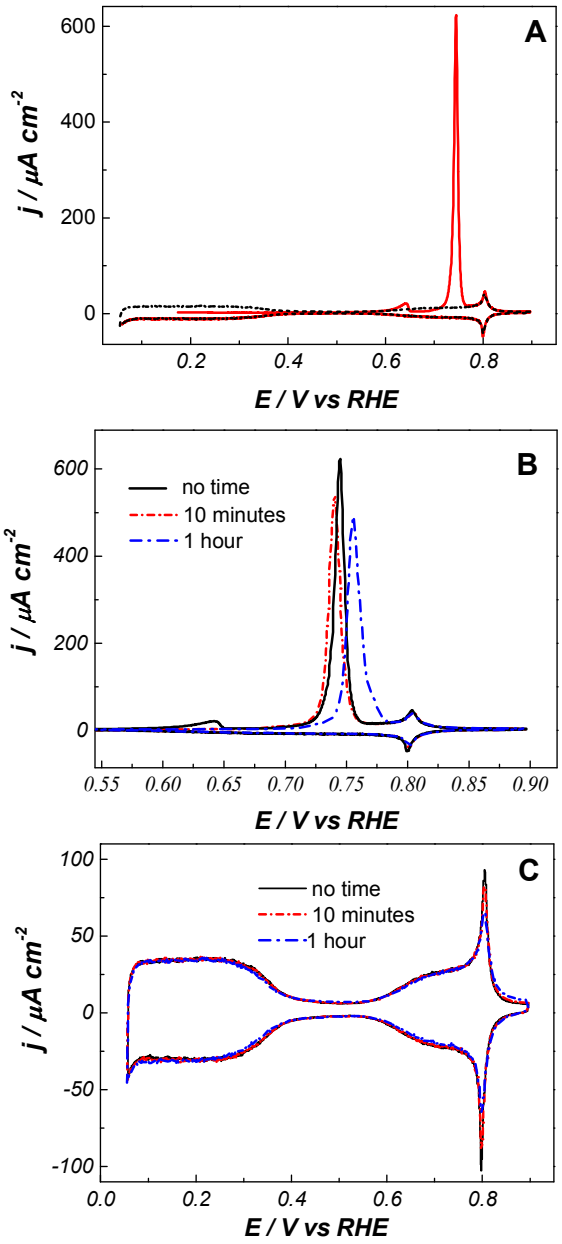

Figure 1. A) CO stripping on Pt(111)|0.1 M $HClO_4$ (solid line) and blank cyclic voltammogram (dashed line), at 20 mV/s. B) CO stripping voltammetric profiles for different Pt(111) delays, at 20 mV/s. C) Blank cyclic voltammograms of the Pt(111)|0.1 M $HClO_4$ after oxidizing the CO, at 50 mV/s.

CO reaction on Pt(111)|[Emmim][Tf_2N] blank solution

After checking the CO oxidation experiment in classical 0.1 M $HClO_4$ test electrolyte, the experimental protocol was investigated in the Pt(111)|[Emmim][Tf_2N] interface. The electrode was pretreated with CO following the procedure stablished in the previous section: The electrode was flame-annealed and cooled down in CO atmosphere. Due to the important moisture sensitivity of the [Emmim][Tf_2N], the Pt(111) electrode was transferred inside the glove box. As the CO monolayer was demonstrated to be stable on Pt(111) even after prolonged exposure to the O_2 containing atmosphere (air), the Pt(111) surface remained covered by CO during the time necessary to introduce the electrode in the glove box. Figure 2A shows the voltammetric CO stripping profile in [Emmim][Tf_2N] liquid, displaying a very sharp peak at 1.1 V vs $Fc^+|Fc$ preceded by less prominent broad peaks (arrows in the figure). After attaining this sharp peak, the scan is reversed to avoid the oxidation of the solvent. The second cycle shows a clear increase of the capacitive current (Figure 2A inset), and no current related to CO oxidation was detected, evidencing that the CO was completely removed during the first scan. The electrochemical window in this second scan was widened as the anodic limit of solvent decomposition is displaced positively. Some broad peaks appear in the capacitive region within -1.0 V and 1.0 V vs Fc/Fc^+ after CO oxidation (inset Figure 2A). By cycling successively within this potential window, these peaks tend to disappear (Figure 2B) and the Pt(111)|Emmim][Tf_2N] interface displays a cyclic voltammogram that is basically a featureless pseudo-capacitance that extends up to 3.5 V. The voltammetric characterization suggests that the origin of the recorded broad peaks in the first scan is related to post-kinetic diffusion controlled reactions after CO oxidation in RTIL. In order to get more insights about the origin of these peaks, cyclic voltammetry experiments were carried out at high speed rate (500 mV/s) to

reduce the diffusion limitation (Figure 2C). The voltammogram displays two oxidation peaks around -0.31 V and 0.06 V, with counterparts at -0.47 V and -0.17 V vs Fc/Fc^+. Similar features were observed and reported in previous publications and assigned to hydrogen (H_2) oxidation and evolution on Pt(111) in contact with [Emmim][Tf_2N][3]. To confirm that the voltammetric peaks in Figure 2C are related with hydrogen reaction on Pt(111), two cyclic voltammograms of Pt(111) in [Emmim][Tf_2N] were recorded, the first one before (black line) and the second one after saturating the RTIL with hydrogen gas (red line, Figure 2D). Figure 2D shows a voltammetric profile for Pt(111)|[Emmim][Tf_2N] that does not contain any singular characteristic feature, obtained after prolonged cycling in this potential window. Only a double layer structure is observed in this case, but analogous peaks to those shown in Figure 2C reappear when the scan was performed in presence of hydrogen in the bulk RTIL electrolyte.

These results strongly support that CO oxidation mechanism in [Emmim][Tf_2N] involves water (water content in the RTIL <10ppm). Then, the proposed mechanism pathway would follow:

$$H_2O + Pt \rightarrow H^+ + Pt\text{-}OH + 1e^- \quad (1)$$

$$Pt\text{-}CO + Pt\text{-}OH \rightarrow Pt + CO_2 + H^+ + 1e^- \quad (2)$$

Protons would then be reduced to hydrogen in the following cycles. The hypothesis is that water could concentrate in the interfacial region at strong surface polarization, and react with CO to produce CO_2, as was proposed in other cases[6, 24]. As the amount of water in the RTIL is very low, these interfacial protons are progressively replaced by the species of the RTIL, which would explain the evolution of the peaks in the blank voltammogram (Figure 2C), that ends up diminishing after successive cycling. These results are not especially surprising, since it was claimed before that CO oxidation to CO_2 in RTIL media necessary involves water presence[6].

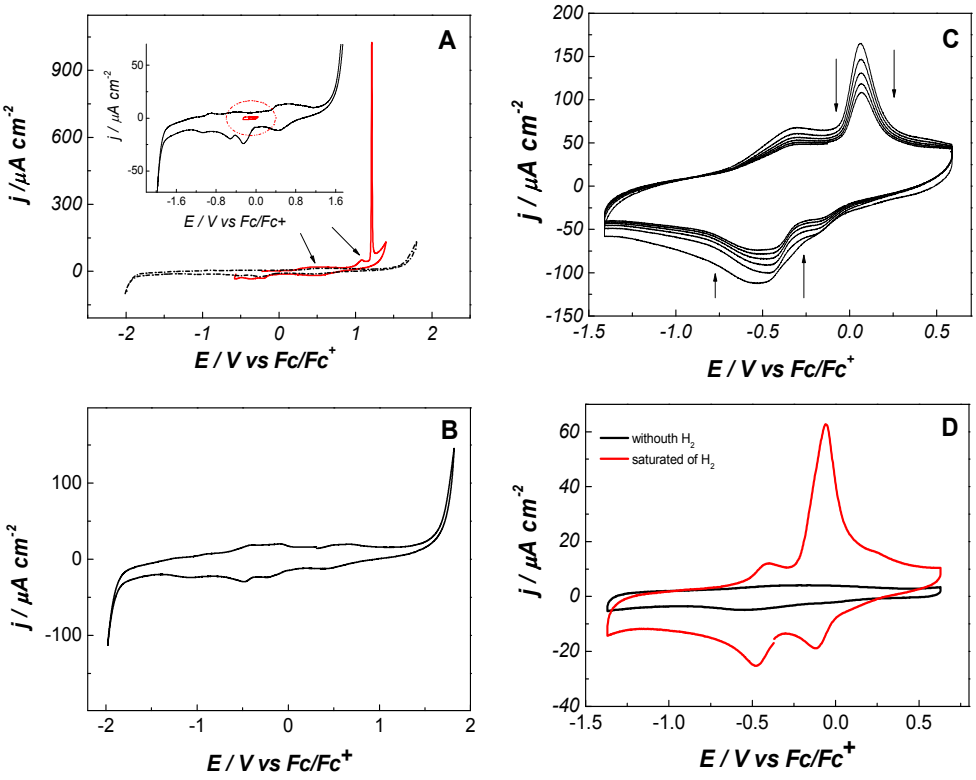

Figure 2. Cyclic voltammograms of the Pt(111) electrode in contact with [Emmim][Tf_2N] blank solution: A) consecutive scans: red solid line: first scan showing the CO stripping, black dashed line: second scan, inset: Blank voltammogram Pt(111)|[Emmim][Tf_2N] (black line) overlapped with CO-Pt(111)|[Emmim][Tf2N] voltammogram (red line). At 20 mV/s. B) Blank cyclic voltammogram of Pt(111)|[Emmim][Tf_2N] at 50 mV/s. C) Blank voltammogram after CO oxidation at 500 mV/s. D) Pt(111)|[Emmim][Tf_2N] cyclic voltammetries: solution saturated to H_2 gas (red line). Blank voltammogram without hydrogen (black line). Scan rate 50 mV/s.

As a further analysis of the CO oxidation result, the involved charge in the voltammetric region of CO stripping was calculated. The obtained value ranges between 700-900 μC cm^{-2} without background subtraction. This value is considerable higher

than the reported in aqueous electrolytes for Pt electrodes, which usually ranges to 320 μC cm^{-2}, after subtracting the double layer and anion adsorption contributions. It must be stressed that the CO coverage must be the same as the one already characterised in aqueous media, since CO adlayer is formed before involving water or IL. The higher value obtained could evidence anion adsorption on the surface on the sites that freed after the oxidation of CO. Similar phenomena were observed in aqueous electrolytes at conditions at which anion adsorption was coupled with CO stripping, and then the apparent charge density associated to the voltammetric CO stripping increased around 437 μC cm^{-2} [25]. It must be highlighted that F.A. Hanc-Scherer et al. investigated similar RTILS but under the presence of thousands of ppm of water[6], and they calculated large CO oxidation charge densities, even higher than 4000 μC cm^{-2}. Authors claimed that CO oxidation was coupled with the oxidation of the RTIL. In the present work, partial oxidation of the IL, overlapped with the CO stripping, could also explain the excess in the charge density but, compared with the results reported in previous works, the oxidation of the solvent appears to be smaller and slightly decoupled from CO oxidation, most likely because of the lowering in water content in the bulk. However, it must be remarked that F.A. Hanc-Scherer et al.[6] integrated a larger potential interval centred at the CO peak oxidation potential, while we have restricted carefully the oxidation potential limit in the voltammetric experiments to avoid the presence of undesirable products in the reverse scan, as well as surface oxidation.

CO reaction on Pt(111)|ChCl:2urea DES blank solution

The proposed procedure to pretreat the Pt(111) was also used with DES. The CO covered electrode was transferred to the cell filled with DES and the voltammetric experiment was performed under Ar atmosphere. Nevertheless, it must be mentioned

that the DES contains around 1% of water at the beginning of the experiments, even after a careful drying procedure under high vacuum[26, 27]. Figure 3 shows the CO oxidation on Pt(111) in DES. The CO oxidation overlaps with the solvent oxidation. The fact that the current density displays hysteresis in the reverse scan (as pointed out by the arrows) evidences that CO is co-oxidized together with the solvent. The solvent oxidation produces some undesirable products that are reduced in the reverse scan (broad peak named as x in Figure 3). Other particularity is that, in the subsequent voltammetric scan, the oxidation onset of the solvent is slightly shifted to less positive potential values, i.e., solvent decomposition is enhanced (Figure 3 inset), likely because CO blockage on Pt(111) was partially eliminated. As a main difference from the behaviour observed in the RTIL, where the electrochemical window was sufficient wide to record completely the oxidation of the CO adlayer, the CO stripping overlaps with the solvent oxidation in the DES. One possibility is that the water present in the DES facilitates its solvent oxidation, reducing the electrochemical window. Another possibility could be that CO is adsorbed on Pt(111) stronger in DES than in [Emmim][Tf_2N]. In order to explore this possibility, attention was paid into the capacitive region.

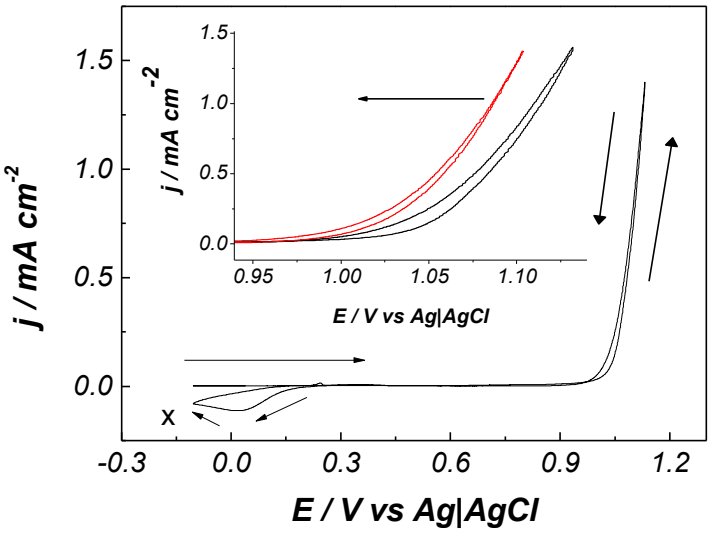

Figure 3. Cyclic voltammograms of the Pt(111) flame annealed and cooled down under CO, in contact with the DES blank solution . The inset shows the first scan (black line) and second scan (red line) at 70ºC. Scan rate 20 mV/s.

Figure 4 shows the voltammetric region between -0.30 and 0.60 V for the CO-Pt(111) in contact with the DES. A group of quasi-reversible broad peaks appear in the double layer region. These new peaks (Figure 4Aa) only appear in DES when the Pt(111) is covered by CO, and they are of unknown origin. By consecutive cycling, these peaks become sharper (Fig. 4Ab) until attain a maximum current value (Fig. 4Ac). However, if successive scans were applied, the current of these peaks decreases monotonically (Fig. 4Ad) and finally disappear leading to a wider pseudo-capacitive voltammetric region (Fig 4Ae). These sharp peaks appear superimposed to a relative constant capacitance of 72 μF cm^{-2}, being the charge involved in the voltammetric region not higher than 50 μC cm^{-2}. The order of magnitude of these values suggests that these peaks could be ascribed to a phase transition involving the interaction of the

adsorbed CO with the species of the DES [28], i.e., these peaks would correspond to solvent network restructuration on the CO-Pt(111) modified surface.

As shown in Figure 4B, the dissolution of the CO causes an increase of the capacitive region (up to 130 mF cm^{-2}). For the purpose of the present work, the interest remains on the fact that adsorbed CO can be removed by successive cycling between indicated potential limits (-0.3 and 0.6 V vs Ag|AgCl). Figure 4C shows the blank cyclic voltammogram of the Pt(111) in contact with the DES after electrochemically removing the CO. The cyclic voltammogram shows a potential window not larger than 2V, shorter than the one displayed by [Emmim][Tf_2N], evidencing the lower electrochemical stability of the DES in comparison with the RTIL. The cyclic voltammogram in the blank solution shows a capacitive region between -0.50 V and 0.70 V vs Ag|AgCl and a group of redox peaks close to the solvent reduction. The couple of redox peaks could be related with the hydrogen reduction-oxidation reaction, as a consequence of the urea (hydrogen bond donor) presence and the residual water in the bulk DES. Similar voltammetric features were previously reported in protic ILs[13, 29]. It is worth to note that cyclic voltammetry recorded in DES, after flame-annealing and cooling the Pt(111) down in the argon atmosphere of the cell (not shown), was virtually identical to that obtained after CO dissolution, confirming that no CO remains in this case on the surface.

From the voltammetric responses of the Pt(111)|IL interface, it is evidenced that reactivity towards the CO oxidation is highly dependent on the employed electrolyte. While in [Emmim][Tf_2N] CO oxidation takes place by reaction with interfacial water, in DES CO strongly interacts with DES species promoting a reorganization in the double layer region. Since this reaction is of paramount interest in terms of sustainability, it deserves special attention and more work is required to establish the parameters that

govern the mechanistic pathway of CO adsorption/oxidation in non-aqueous electrolytes. For the purposes of the present work, CO has been revealed as an useful tool to keep clean and ordered the Pt(111) surface in contact with both RTIL and DES.

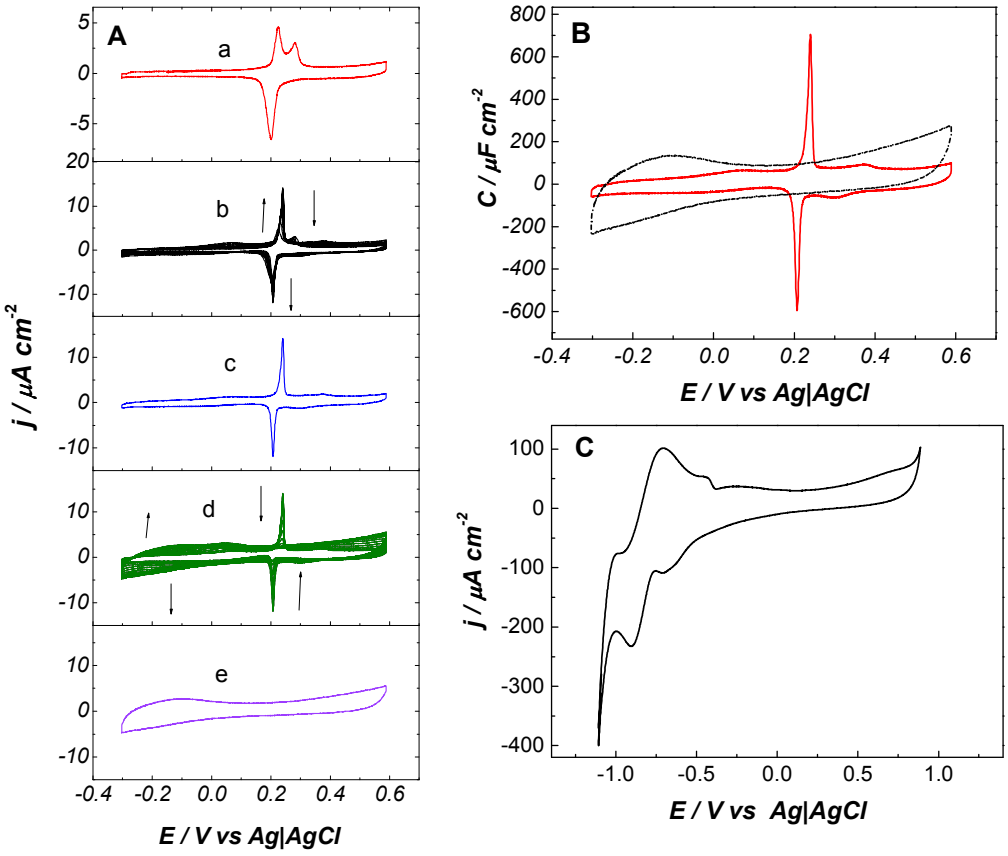

Figure 4. Cyclic voltammograms of the Pt(111)|DES interface at 70ºC: A) consecutive scans in the double layer region when the Pt(111) is covered by CO. B) double layer region when. Pt(111) is covered by CO (red solid line) and Pt is free of CO (black dashed line). Scan rate 20 mV/s. C) blank cyclic voltammogram at 50 mV/s for a Pt(111) CO-free.

Ni deposition on Pt(111) in the ILs

Nickel electrodeposition in [Emmim][Tf_2N] was investigated on Pt(111) pretreated with CO. Taking advantage from the fact that the RTIL shows a large electrochemical window, the CO stripping was carried out in the same solution containing 0.05 M Ni[Tf_2N]$_2$ + [Emmim][Tf_2N], followed by successive cycling in the double layer region until reaching a stationary profile. Figure 5A shows the cyclic voltammetry for the nickel deposition on Pt(111) overlapped with the blank cyclic voltammogram. The voltammetric window allows the Ni deposition with negligible solvent co-reduction, although quite negative applied potentials are required for nickel electrodeposition. In addition, the Ni(II) reduction/dissolution is a very irreversible process and around 1V separates the onset of the nickel reduction and the onset of the nickel oxidation. Similar results were reported by Katayama et. al using other RTILs based on the [Tf_2N] anion[30]. The authors attributed the high irreversibility of the process to the particular nature of the Metal|IL interface. The presence of the cation (a large-size organic ion) on the surface at those negative potentials would hinder the electron transfer between the metal precursor (Ni(II)) and Pt(111). So, high overpotential is needed to overcome this energetic barrier. The irreversibility of the process could be also due to the slow restructuration of the solvent network in the reverse direction of the scan or be related to the inert condition of nickel towards its deposition that is also observed in aqueous medium[31-33].

Figure 5B shows the chronoamperometric transient of Ni(II) deposition at -0.70 V vs Fc/Fc^+. The j-t transient shows a slow current increase until a maximum is attained around at 150s, just evidencing the slowness of the process. Then, the current falls down with time. The profile of the recorded j-t transient suggests that the nickel nucleates and grows under diffusion control (3-D nucleation and mass controlled growth mechanism).

At first, this nickel deposits prepared onto Pt(111) at low applied overpotentials conditions were analysed. Figure 5C shows the FE-SEM image corresponding to the nickel deposit onto Pt(111). Under these conditions, nickel nanoclusters are formed homogeneously covering the entire surface (sized <100 nm) without evidencing any grade of porosity (Figure 5D). The absence of holes or porosity supports that nickel deposition takes place without the interference of the solvent reduction under these conditions. The EDS analysis carried on a Pt polycrystalline bead sample modified with low coverages of Ni, confirmed the presence of Ni (Figure S1) but also showed the presence of low oxygen content, compatible with surface oxidation in the environment of the sample cleaning after removing it from the solution.

Applying slightly higher overpotentials to enhance the rate of Ni deposition and then increasing the Ni coverage on Pt, result in the formation of a black powdery deposit with low adherence. In addition, the XPS analysis of these deposits (Figure S2) showed the presence of different Ni oxide and Ni hydroxide species as well as metallic Ni. The presence of NiO/NiOxHy could be due to the fact that the grains of Ni are of nanometric size (as the FE-SEM showed) and easily oxidized by the environment. Another possibility is that the low interfacial water content could be co-reduced together with the Ni favouring the appearance of oxygenated Ni species. At moderate higher applied overpotentials (Eap>-1.2V vs Fc+/Fc), Ni deposits on Pt had not sufficient adherence and the deposit was lost in the bulk RTIL. It is worth to say that Katayama et al. observed the formation of nanoparticles which could not adhere to the surface and keep growing, then losing the deposit. In these works, Katayama et al. argued that the presence of the ionic species in the interfacial region, especially the presence of the cation, inhibited the growth of the deposit favouring nanostructures with low adherence[31, 34]. These results show that [Emmim][Tf_2N] allows modifying Pt surface

with low amount of Ni but the process is limited to a narrow potential range (E<-1.0V vs Fc+/Fc) due to the low adherence of the prepared deposits as well the appearance of oxygenated Ni species.

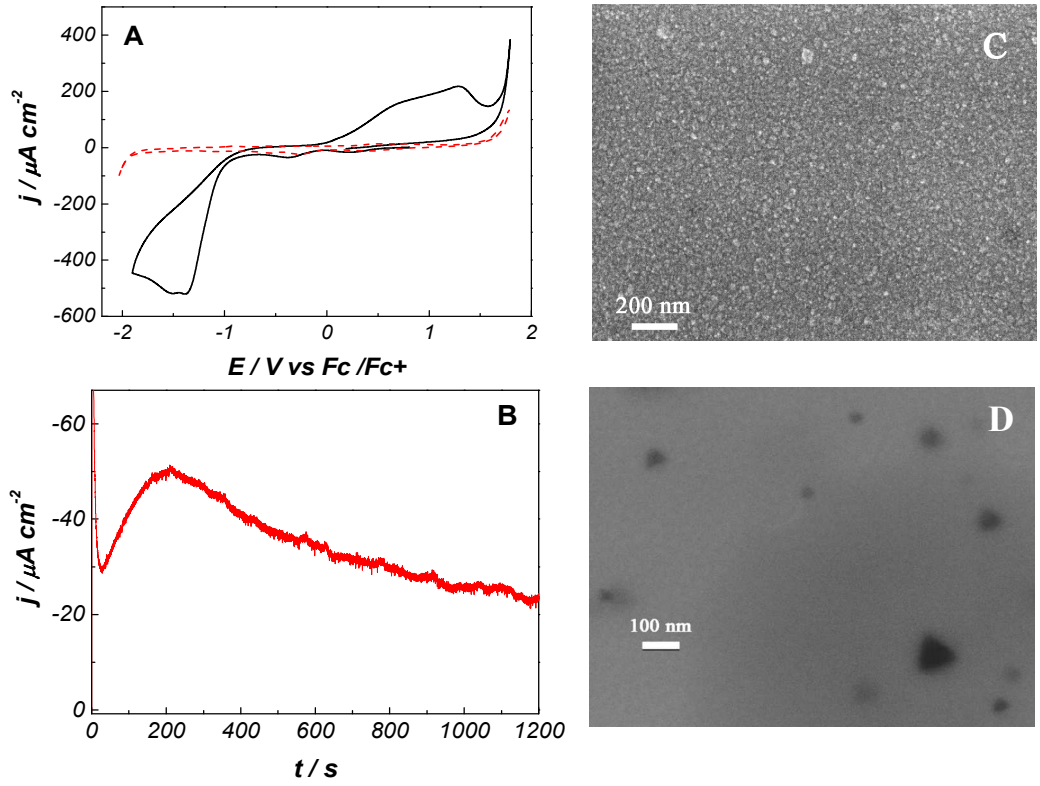

Figure 5. A) Cyclic voltammogram at 20 mV/s of the nickel deposition in 50mM $Ni[Tf_2N]_2$+[Emmim][Tf_2N] solution. The dashed line corresponds to the blank. B) j-t transient recorded at -0.700V. C) FE-SEM image of nickel deposit obtained at -40 mC cm^2 at -0.70V. D) FE-SEM bare Pt(111).

Before investigating Ni(II) deposition in DES, a temperature study was carried out, from which 0.1 M Ni(II) at 70ºC were selected as the optimal conditions to perform Ni(II) deposition on the Pt electrode (Figure S3). The high viscosity of the media hinders the Ni(II) deposition at lower temperatures. An increase of the nickel (II)

concentration (twice that the employed in the RTIL) was also employed in order to increase the deposition rate.

Figure 6A shows the cyclic voltammogram for 0.1M Ni(II) electrodeposition on Pt(111) in DES. The dashed line corresponds to the blank cyclic voltammetry within the potential limits where the nickel electrodeposition was carried out. Although the electrochemical window of the DES is considerable shorter than in [Emmim][Tf_2N], it is sufficiently large to allow the nickel deposition. When the nickel deposit is present on the Pt(111) surface, the lower potential limit for the DES reduction shift to lower potentials because nickel is less catalytic. The solvent reduction involves hydrogen reaction (broad peak labelled as x' in the anodic scan of the Pt(111)|DES cyclic voltammogram)[35-37].

The cyclic voltammetry from the Ni deposition shows two reduction peaks in the negative scan (a and b) thus suggesting a change in the nickel deposition mechanism. As we demonstrated in our previous report[27], these two peaks are related with different hydrogenated Ni species, i.e. Ni containing different fractions of hydrogen in its network (α-Ni and β-Ni)[37, 38]**.** In addition we also showed that surface passivation started at higher applied overpotentials near to the onset of solvent bulk reduction. In order to minimize solvent co-reduction (Figure 6B) and avoid surface passivation, chronoamperometric transients were recorded at low applied overpotentials. As in RTIL, the j-t transient evidences nucleation and growth mechanism (Figure 6B), being the maximum current value centred at around 100 s, showing that the growth in this media is also kinetically slow.

Ni nanostructures obtained in DES have a size that approaches to 100 nm but they are higher than those obtained in [Emmim][Tf_2N], although the sample has been prepared under the same deposition charge for comparison (Figure 6C). The Ni deposit

in DES is also homogenous and no traces of porosity due to solvent co-reduction are observed even in the case which lower potentials were applied. The EDS analysis carried at similar applied overpotentials (Figure S4), detected the presence of Ni and a negligible fraction of oxygen.

All these results evidence the influence of the electrolyte. The tuning of the Ni decoration seems possible modulating the electrodeposition conditions in the selected IL medium.

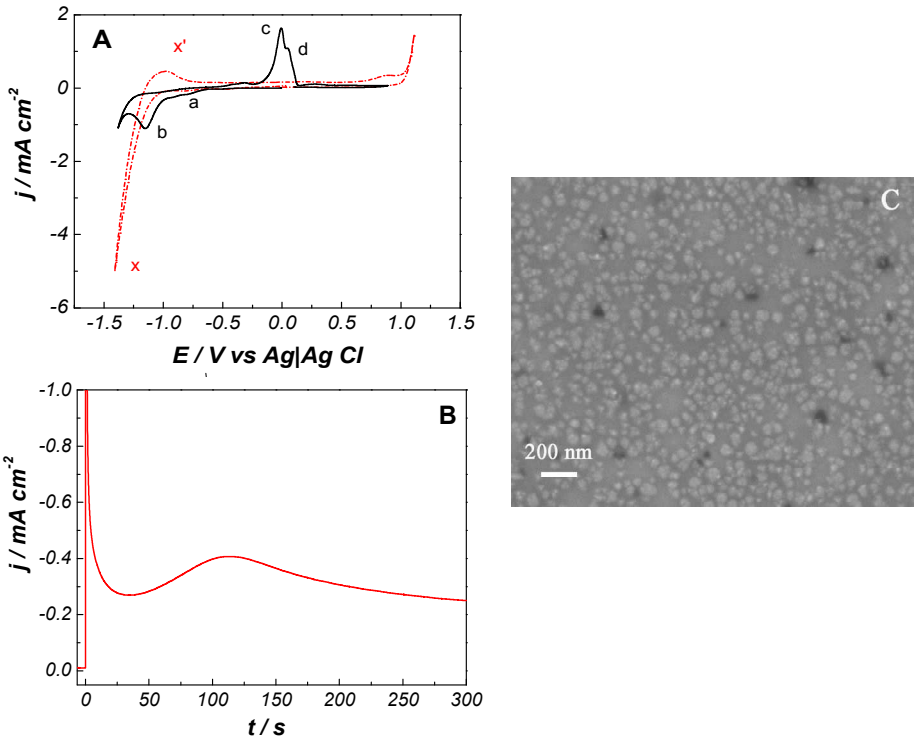

Figure 6. A) Cyclic voltammogram of the nickel deposition on Pt(111) from a 0.1 M $NiCl_2$ + DES solution. The dashed line corresponds to the blank cyclic voltammogram at 20 mV/s. B) j-t transient recorded at -1.0 V. C) FE-SEM image of the Ni deposit obtained at -0.98V and -40 mC cm^{-2}.

CONCLUSIONS

An strategy to pretreat the Pt(111) substrate ensuring both surface ordering and cleanness in IL media was proposed. The method involves the protection of the surface with CO, and later stripping of the CO electrochemically to CO_2. The used RTIL presents an electrochemical window that allows the neat CO stripping within the potential limits, but the DES has not enough potential window and the CO oxidation overlaps with the oxidation of the solvent. In the RTIL, the low amount of water impurities promotes the CO oxidation, but in the DES, the CO strongly interacts with species of the DES and cannot be oxidized at moderate applied potentials. In addition, the cyclic voltammetry of the CO-Pt(111)|DES interface displays a couple of sharp peaks in the capacitive zone. These peaks were associated to solvent restructuration processes involving the CO adsorbed on Pt(111). The CO does not remain stable if a large number of consecutive cycles is carried out. These results show the complexity of CO reactivity on Pt in IL media. Different parameters may govern the pathway reaction mechanism, including the different properties of the interfacial Pt|IL region that highly influence the CO oxidation reaction. However, for the goal of this work, CO is confirmed to be a valuable tool to protect the surface and can be used in IL media to investigate platinum single crystal electrodes, keeping the desired surface ordering.

Once demonstrated that CO allows obtaining reliable blank cyclic voltammograms of Pt(111) in contact with both DES and [Emmim][Tf_2N] liquids as a hallmark of the accurate state of the electrode, the applicability of these two ionic liquid media to modify Pt(111) with Ni was evaluated. Both ILs have shown chemical differences that influence the nickel deposition in several ways. The voltammetric study showed that the [Emmim][Tf_2N] has a potential window sufficiently wide for the nickel electrodeposition, but low adherent Ni deposits are obtained even under moderate

applied overpotentials. The modification of the Pt surfaces with low Ni coverages can be carried out, but the low potential range available for that reduces considerably the applicability. At low applied overpotentials in the RTIL, nanostructures of nickel with size smaller than 100 nm can be obtained. On the other hand, the DES is less electrochemically stable and both higher nickel(II) concentration and temperature are needed to overcome the effect of its higher viscosity. The reduction of the solvent overlaps with the Ni deposition, but the Ni(II)-solvent co-reduction can be minimized applying lower potentials, conditions at which Ni nanostructures were obtained, slightly bigger than those in the RTIL. In summary, although [Emmim][Tf_2N] has a wider potential window for Ni deposition this is not exploitable due to the low quality of the obtained deposits which lack of adherence even at moderate applied overpotentials. However, ChCl:2urea DES was found to be a good candidate for the surface modification due to the best quality of the deposited coatings.

AUTHOR INFORMATION

Corresponding Author

*E-mail: paula.sebastian@ua.es

*E-mail: juan.feliu@ua.es

ORCID

Paula Sebastián: 0000-0001-7985-0750

Juan M. Feliu: 0000-0003-4751-3279

Yang Shao-Horn: 0000-0001-8714-2121

Elvira Gómez: 0000-0002-9223-6357

Victor Climent: 0000-0002-2033-5284

Author Contributions

The manuscript was written through contributions of all authors. All authors have given approval to the final version of the manuscript.

Notes

The authors declare no competing financial interest.

SUPPORTING INFORMATION AVAILABLE

ACKNOWLEDGMENTS

This work has been financially supported by the MCINN-FEDER (Spain) through the projects: CTQ2016-76221-P and TEC2017-85059-C3-2R. P. Sebastian acknowledges to MECD the award of a FPU grant.

REFERENCES

(1) Montiel, M.; Solla-Gullón, J.; Sánchez-Sánchez, C., Electrochemical Reactivity and Stability of Platinum Nanoparticles in Imidazolium-Based Ionic Liquids. *J. Solid State Electrochem.* **2015**, 1-10.

(2) Navarro-Suarez, A. M.; Hidalgo-Acosta, J. C.; Fadini, L.; Feliu, J. M.; Suarez-Herrera, M. F., Electrochemical Oxidation of Hydrogen on Basal Plane Platinum Electrodes in Imidazoliurn Ionic Liquids. *J. Phys. Chem. C* **2011,** *115* (22), 11147-11155.

(3) Sandoval, A. P.; Suarez-Herrera, M. F.; Feliu, J. M., Hydrogen Redox Reactions in 1-Ethyl-2,3-Dimethylimidazolium Bis(Trifluoromethylsulfonyl)Imide on Platinum Single Crystal Electrodes. *Electrochem. Commun.* **2014,** *46*, 84-86.

(4) Sebastián, P.; Sandoval, A. P.; Climent, V.; Feliu, J. M., Study of the Interface Pt(111)/ [Emmim][NTF_2] Using Laser-Induced Temperature Jump Experiments. *Electrochem. Commun.* **2015,** *55*, 39-42.

(5) Hanc-Scherer, F. A.; Montiel, M. A.; Montiel, V.; Herrero, E.; Sanchez-Sanchez, C. M., Surface Structured Platinum Electrodes for the Electrochemical Reduction of Carbon Dioxide in Imidazolium Based Ionic Liquids. *Phys.Chem.Chem.Phys.* **2015,** *17* (37), 23909-23916.

(6) Hanc-Scherer, F. A.; Sanchez-Sanchez, C. M.; Ilea, P.; Herrero, E., Surface-Sensitive Electrooxidation of Carbon Monoxide in Room Temperature Ionic Liquids. *ACS Catal.* **2013,** *3* (12), 2935-2938.

(7) Clavilier, J.; Faure, R.; Guinet, G.; Durand, R., Preparation of Monocrystalline Pt Microelectrodes and Electrochemical Study of the Plane Surfaces Cut in the Direction of the {111} and {110} Planes. *J.Electroanal. Chem.* **1980,** *107* (1), 205-209.

(8) Kibler, L. A.; Cuesta, A.; Kleinert, M.; Kolb, D. M., In-Situ STM Characterisation of the Surface Morphology of Platinum Single Crystal Electrodes as a Function of Their Preparation. *J. Electroanal. Chem.* **2000,** *484* (1), 73-82.

(9) Feliu, J. M.; Orts, J. M.; Femandez-Vega, A.; Aldaz, A.; Clavilier, J., Electrochemical Studies in Sulphuric Acid Solutions of Adsorbed CO on Pt (111) Electrodes. *J. Electroanal. Chem.* **1990,** *296* (1), 191-201.

(10) Climent, V.; Feliu, J. M., Thirty Years of Platinum Single Crystal Electrochemistry. *J. Solid State Electrochem.* **2011,** *15* (7), 1297.

(11) Clavilier, J.; Albalat, R.; Gomez, R.; Orts, J. M.; Feliu, J. M.; Aldaz, A., Study of the Charge Displacement at Constant Potential During CO Adsorption on Pt(110) and Pt(111) Electrodes in Contact with a Perchloric Acid Solution. *J. Electroanal. Chem.* **1992,** *330* (1), 489-497.

(12) Attard, G. A.; Hunter, K.; Wright, E.; Sharman, J.; Martínez-Hincapié, R.; Feliu, J. M., The Voltammetry of Surfaces Vicinal to Pt{110}: Structural Complexity Simplified by CO Cooling. *J. Electroanal. Chem.* **2017,** *793*, 137-146.

(13) Ejigu, A.; Walsh, D. A., The Role of Adsorbed Ions During Electrocatalysis in Ionic Liquids. *J. Phys. Chem. C* **2014,** *118* (14), 7414-7422.

(14) Zhang, Q.; Wang, Q.; Zhang, S.; Lu, X.; Zhang, X., Electrodeposition in Ionic Liquids. *ChemPhysChem* **2016,** *17* (3), 335-351.

(15) Abbott, A. P.; McKenzie, K. J., Application of Ionic Liquids to the Electrodeposition of Metals. *Phys.Chem.Chem.Phys.* **2006,** *8* (37), 4265-4279.

(16) Subbaraman, R.; Tripkovic, D.; Chang, K.-C.; Strmcnik, D.; Paulikas, A. P.; Hirunsit, P.; Chan, M.; Greeley, J.; Stamenkovic, V.; Markovic, N. M., Trends in Activity for the Water Electrolyser Reactions on 3d M(Ni,Co,Fe,Mn) hydr(oxy)oxide catalysts. *Nat. Mater.* **2012,** *11*, 550..

(17) Stamenkovic, V. R.; Fowler, B.; Mun, B. S.; Wang, G.; Ross, P. N.; Lucas, C. A.; Markovic, N. M., Improved Oxygen Reduction Activity on Pt_3/Ni(111) Via Increased Surface Site Availability. *Science* **2007**.

(18) Ledezma-Yanez, I.; Wallace, W. D. Z.; Sebastián-Pascual, P.; Climent, V.; Feliu, J. M.; Koper, M. T. M., Interfacial Water Reorganization as a Ph-Dependent Descriptor of the Hydrogen Evolution Rate on Platinum Electrodes. *Nat. Energy* **2017,** *2* (4).

(19) Gnahm, M.; Kolb, D. M., The Purification of an Ionic Liquid. *J. Electroanal. Chem.* **2011,** *651* (2), 250-252.

(20) Abbott, A. P.; Boothby, D.; Capper, G.; Davies, D. L.; Rasheed, R. K., Deep Eutectic Solvents Formed between Choline Chloride and Carboxylic Acids: Versatile Alternatives to Ionic Liquids. *J. Am. Chem. Soc.* **2004,** *126* (29), 9142-9147.

(21) Clavilier, J., The Role of Anion on the Electrochemical Behaviour of a {111} Platinum Surface; an Unusual Splitting of the Voltammogram in the Hydrogen Region. *J. Electroanal. Chem.* **1979,** *107* (1), 211-216.

(22) Suchorski, Y.; Drachsel, W.; Rupprechter, G., High-Field Versus High-Pressure: Weakly Adsorbed CO Species on Pt(111). *Ultramicroscopy* **2009,** *109* (5), 430-435.

(23) Farias, M. J. S.; Busó-Rogero, C.; Gisbert, R.; Herrero, E.; Feliu, J. M., Influence of the CO Adsorption Environment on Its Reactivity with (111) Terrace Sites in Stepped Pt Electrodes under Alkaline Media. *J. Phys. Chem. C* **2014,** *118* (4), 1925-1934.

(24) Figueiredo, M. C.; Ledezma-Yanez, I.; Koper, M. T. M., In Situ Spectroscopic Study of CO_2 Electroreduction at Copper Electrodes in Acetonitrile. *ACS Catal.* **2016,** *6* (4), 2382-2392.

(25) Carol Korzeniewski, V. C., and Juan M. Feliu, Electrochemistry at Pt Single Crystal Electrodes, Chapter Book, Electroanalytical Chemistry. In *Electroanalytical Chemistry. A Series of Advances*, CRC Press: 2011; Vol. 75.

(26) Du, C.; Zhao, B.; Chen, X.-B.; Birbilis, N.; Yang, H., Effect of Water Presence on Choline Chloride-2urea Ionic Liquid and Coating Platings from the Hydrated Ionic Liquid. *Sci. Reports* **2016,** *6*, 29225.

(27) Sebastian, P.; Giannotti, M. I.; Gómez, E.; Feliu, J. M., Surface Sensitive Nickel Electrodeposition in Deep Eutectic Solvent. *ACS Appl. Energy Mater.* **2018,** *1 (3), 1016-1028.* .

(28) Sebastián, P.; Climent, V.; Feliu, J. M., Characterization of the Interfaces between Au(hkl) Single Crystal Basal Plane Electrodes and [Emmim][Tf_2N] Ionic Liquid. *Electrochem. Commun.* **2016,** *62*, 44-47.

(29) Greaves, T. L.; Drummond, C. J., Protic Ionic Liquids: Properties and Applications. *Chem. Rev.* **2008,** *108* (1), 206-237.

(30) Zhu, Y. L.; Kozuma, Y.; Katayama, Y.; Miura, T., Electrochemical Behavior of Ni(II)/Ni in a Hydrophobic Amide-Type Room-Temperature Ionic Liquid. *Electrochim. Acta* **2009,** *54* (28), 7502-7506.

(31) Katayama, Y.; Fukui, R.; Miura, T., Electrodeposition of Cobalt from an Imide-Type Room-Temperature Ionic Liquid. *J. Electrochem. Soc.* **2007,** *154* (10), D534-D537.

(32) Tułodziecki, M.; Tarascon, J. M.; Taberna, P. L.; Guéry, C., Importance of the Double Layer Structure in the Electrochemical Deposition of Co from Soluble Co^{2+} Based Precursors in Ionic Liquid Media. *Electrochim. Acta* **2014,** *134*, 55-66.

(33) Tułodziecki, M.; Tarascon, J. M.; Taberna, P. L.; Guéry, C., Non-Equilibrium Ionic Liquid-Electrode Interface at Elevated Temperature and Its Influence on Co^{2+} Reduction Process. *J. Electrochem. Soc.* **2016,** *163* (8), D355-D365.

(34) Katayama, Y.; Oshino, Y.; Ichihashi, N.; Tachikawa, N.; Yoshii, K.; Toshima, K., Electrochemical Preparation of Palladium Nanoparticles in Bis(Trifluoromethylsulfonyl)Amide Ionic Liquids Consisting of Pyrrolidinium Cations with Different Alkyl Chain Lengths. *Electrochim. Acta* **2015,** *183*, 37-41.

(35) Laursen, A. B.; Varela, A. S.; Dionigi, F.; Fanchiu, H.; Miller, C.; Trinhammer, O. L.; Rossmeisl, J.; Dahl, S., Electrochemical Hydrogen Evolution: Sabatier's Principle and the Volcano Plot. *J. Chem. Educ.* **2012,** *89* (12), 1595-1599.

(36) Lazarescu, V.; Clavilier, J., Ph Effects on the Potentiodynamic Behavior of the Pt(111) Electrode in Acidified $NaClO_4$ Solutions. *Electrochim. Acta* **1998,** *44* (6–7), 931-941.

(37) Mernissi Cherigui, E. A.; Sentosun, K.; Bouckenooge, P.; Vanrompay, H.; Bals, S.; Terryn, H.; Ustarroz, J., Comprehensive Study of the Electrodeposition of Nickel Nanostructures from Deep Eutectic Solvents: Self-Limiting Growth by Electrolysis of Residual Water. *J. Phys. Chem. C* **2017,** *121* (17), 9337-9347.

(38) Gómez, E.; Pollina, R.; Vallés, E., Nickel Electrodeposition on Different Metallic Substrates. *J. Electroanal. Chem.* **1995,** *386* (1-2), 45-56.

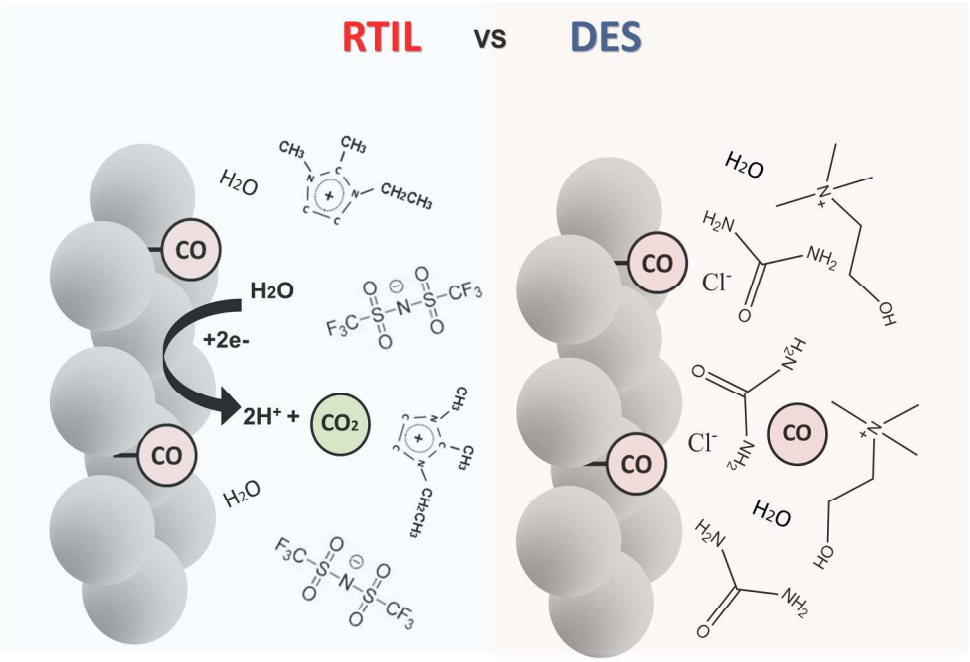

Table of Contents graphic

224x215mm (300 x 300 DPI)

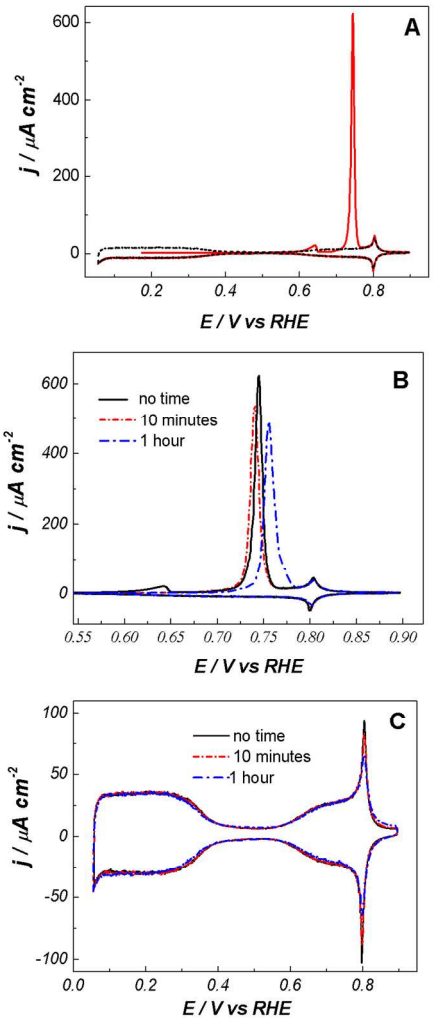

Figure 1

Figure 1. A) CO stripping on Pt(111)|0.1 M HClO4 (solid line) and blank cyclic voltammogram (dashed line), at 20 mV/s. B) CO stripping voltammetric profiles for different Pt(111) delays, at 20 mV/s. C) Blank cyclic voltammograms of the Pt(111)|0.1 M HClO4 after oxidizing the CO, at 50 mV/s.

150x262mm (300 x 300 DPI)

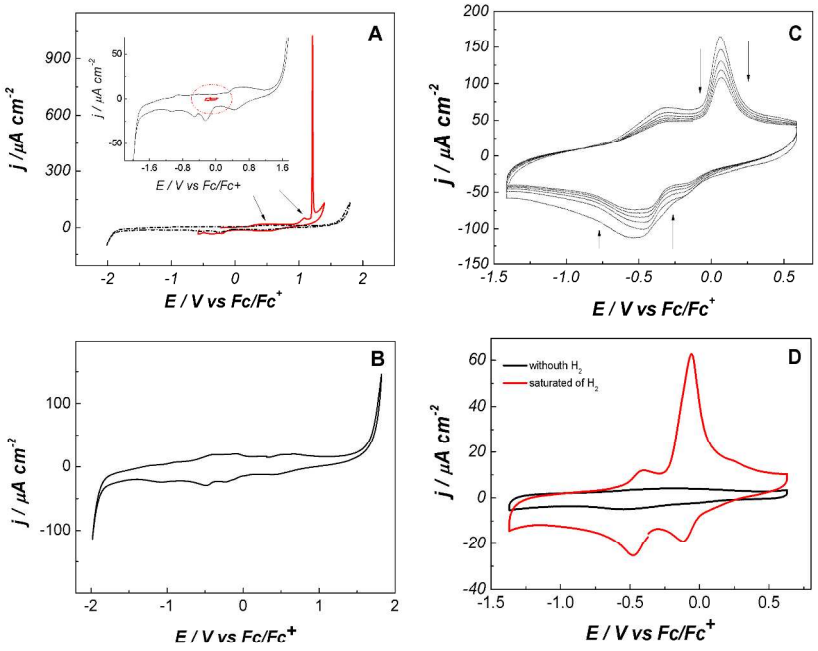

Figure 2

Figure 2. Cyclic voltammograms of the Pt(111) electrode in contact with [Emmim][Tf2N] blank solution: A) consecutive scans: red solid line: first scan showing the CO stripping, black dashed line: second scan, inset: Blank voltammogram Pt(111)|[Emmim][Tf2N] (black line) overlapped with CO-Pt(111)|[Emmim][Tf2N] voltammogram (red line). At 20 mV/s. B) Blank cyclic voltammogram of Pt(111)|[Emmim][Tf2N] at 50 mV/s. C) Blank voltammogram after CO oxidation at 500 mV/s. D) Pt(111)|[Emmim][Tf2N] cyclic voltammetries: solution saturated to H2 gas (red line). Blank voltammogram without hydrogen (black line). Scan rate 50 mV/s.

1000x800mm (78 x 78 DPI)

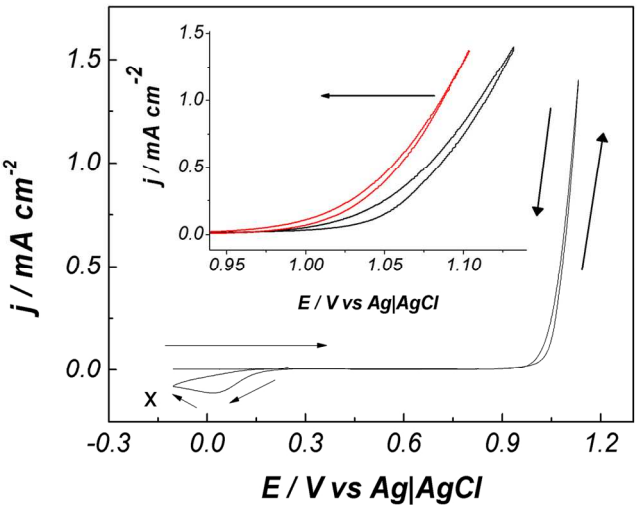

Figure 3

Figure 3. Cyclic voltammograms of the Pt(111) flame annealed and cooled down under CO, in contact with the DES blank solution . The inset shows the first scan (black line) and second scan (red line) at 70ºC. Scan rate 20 mV/s.

150x119mm (300 x 300 DPI)

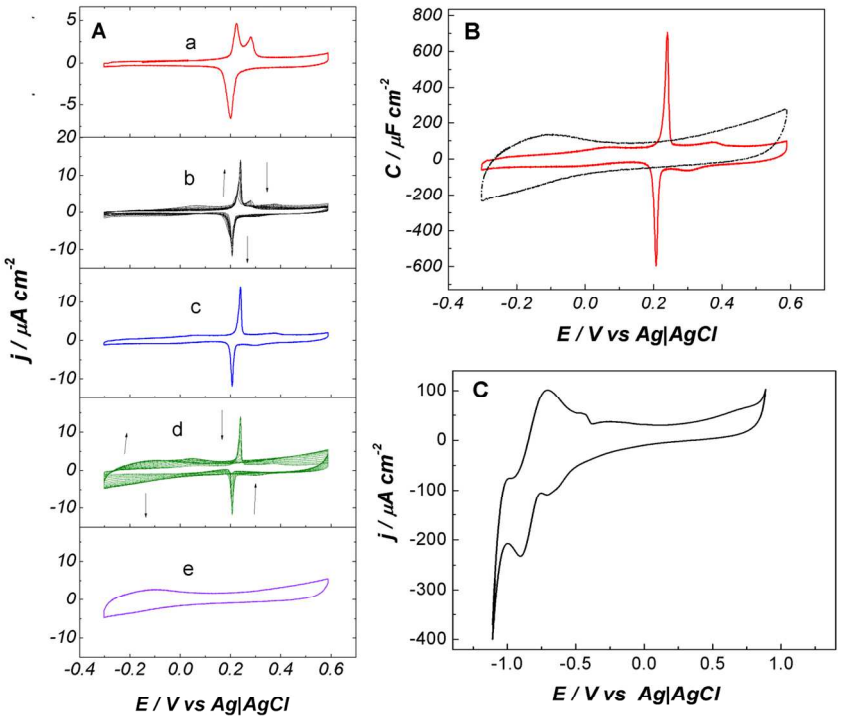

Figure 4

Figure 4. Cyclic voltammograms of the Pt(111)|DES interface at 70ºC: A) consecutive scans in the double layer region when the Pt(111) is covered by CO. B) double layer region when. Pt(111) is covered by CO (red solid line) and Pt is free of CO (black dashed line). Scan rate 20 mV/s. C) blank cyclic voltammogram at 50 mV/s for a Pt(111) CO-free.

150x119mm (300 x 300 DPI)

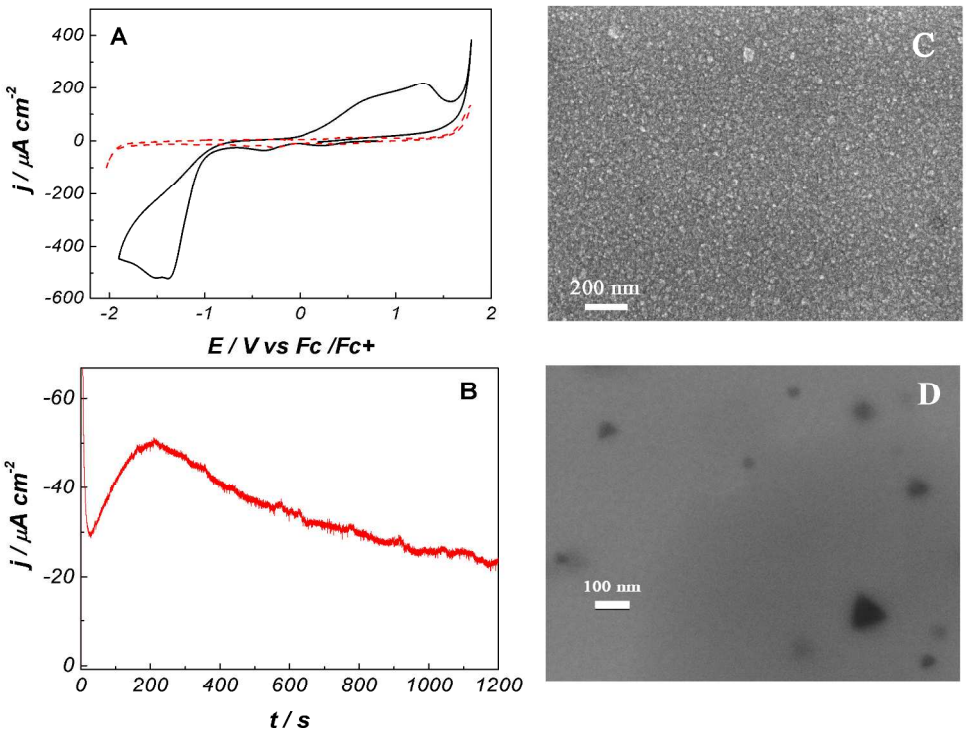

Figure 5

Figure 5. A) Cyclic voltammogram at 20 mV/s of the nickel deposition in 50mM Ni[Tf2N]2+[Emmim][Tf2N] solution. The dashed line corresponds to the blank. B) j-t transient recorded at -0.700V. C) FE-SEM image of nickel deposit obtained at -40 mC cm2 at -0.70V. D) FE-SEM bare Pt(111).

1000x800mm (78 x 78 DPI)

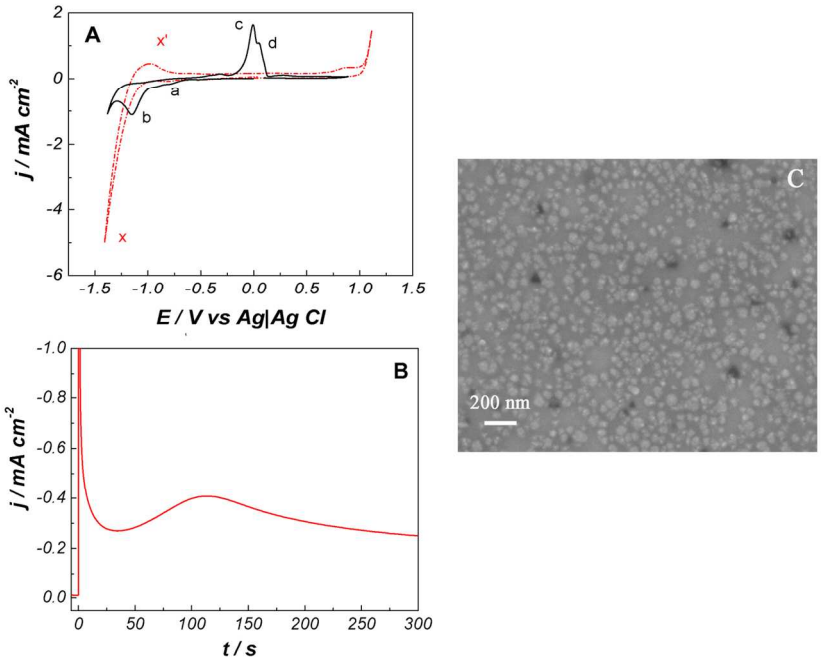

Figure 6

Figure 6. A) Cyclic voltammogram of the nickel deposition on Pt(111) from a 0.1 M NiCl2 + DES solution. The dashed line corresponds to the blank cyclic voltammogram at 20 mV/s. B) j-t transient recorded at -1.0 V. C) FE-SEM image of the Ni deposit obtained at -0.98V and -40 mC cm-2.

150x119mm (300 x 300 DPI)